

Surface melting of nodular cast iron by Nd-YAG laser and TIG

K.Y. Benyounis^{a,*}, O.M.A. Fakron^b, J.H. Abboud^b, A.G. Olabi^c, M.J.S. Hashmi^c

^a Department of Industrial Engineering, Faculty of Engineering, Garyounis University, P.O. Box 1308, Benghazi, Libya

^b Department of Mechanical Engineering, Faculty of Engineering, Garyounis University, P.O. Box 1308, Benghazi, Libya

^c School of Mechanical & Manufacturing Engineering, DCU, Dublin 9, Ireland

Received 23 August 2004; received in revised form 25 April 2005; accepted 26 April 2005

Abstract

The effect of surface melting and rapid solidification on the structure and hardness of nodular cast iron has been investigated. Two heat sources were used for surface melting mainly, laser beam (LB) and electric arc generated between the tungsten electrode and the specimen (i.e. TIG). Optical microscope, scanning electron microscope and X-ray diffraction were used to describe the microstructure and identify the phases in the melted zone. Results showed that surface melting has led to a complete dissolution of the graphite nodules and re-solidification of a dendritic structure. The specimen melted by TIG showed dendrites of transformed austenite in a matrix of eutectic consisting of transformed austenite γ and Fe_3C while the laser-melted zone exhibited finer dendrites of retained austenite surrounded by a continuous network of Fe_3C ; some needles of martensite within the dendrites are observed. The retained austenite dendrites have a preferred growth direction and contained a high concentration of dissolved carbon. The microhardness of the nodular cast iron was found to be significantly increased after melting. © 2005 Elsevier B.V. All rights reserved.

Keywords: Nd-YAG laser and TIG; Nodular cast iron; Microhardness; X-ray diffraction

1. Introduction

Cast irons are important ferrous metals widely used in the manufacture of machine tool beds, cams, pistons, cylinders, etc., because of their low cost and desirable properties like low melting point, good fluidity and cast-ability, excellent machinability, good wear resistance and good mechanical properties [1]. However, under severe service conditions their performance and reliability can be limited by various forms of wear including erosion. One of the alternative ways to improve erosion is to add alloying elements but this solution increases material cost and also increases the consumption of the alloying elements.

The availability of high power lasers have led to develop new methods in surface hardening suitable to cast irons [2,3]. One of the processes is the laser surface melting and sub-

sequent solidification. In this process, the metal surface is melted while the cold substrate ensures rapid cooling (self-quenching by conduction). The rapid solidification and the quenching process give the microstructure its distinct properties. Cooling rates as high as 10^6 °C/s are affected compared to less than 10^2 °C/s in conventional solidification by casting. This in turn has several metallurgical advantages such as refinement of the microstructure, extension of solid solubility and production of an amorphous structure or meta-stable phases if the cooling rate is too high. This treatment will lead to increase hardness and other related properties. The technique of laser surface melting has been applied to a number of alloys such as carbon steel [4], stainless steels [5], titanium alloys [6], nickel-based alloys [7] and aluminium alloys [8]. Significant changes in the structure and properties of the treated surface were reported. The aim of this work was to use a concentrated laser beam emitted from the Nd-YAG for surface melting of the nodular cast iron. The rapid cooling of the melted zone enables the formation of the white cast iron, which is very hard and wear resistant, on the surface of the nodular cast iron. Some

* Corresponding author.

E-mail addresses: kybenyounis@yahoo.com (K.Y. Benyounis), jhabboud@yahoo.com (J.H. Abboud), abdul.olabi@dcu.ie (A.G. Olabi), salem.hashmi@dcu.ie (M.J.S. Hashmi).

results of surface melting by TIG are also presented for comparison.

2. Experimental procedure

The chemical composition of the nodular cast iron used is: 3.58 wt.% C, 0.22 wt.% Mn, 0.05 wt.% P, 0.039 wt.% Mg, 0.006 wt.% S and Fe balance. Samples of 20 mm long, 20 mm wide and 12.5 mm thick were cut from sheet stock and surface ground mechanically, polished and etched with nital to decrease the laser beam reflectivity.

A solid state Nd-YAG laser of 1.06 μm wavelength and maximum power 100 W was used to melt the specimen's surface. The beam mode used was gassion. A series of experiments was carried out using different pulse durations and power densities. Some specimens were melted by electric arc generated between the tungsten electrode and the specimen using currents ranged between 80 and 120 A and the voltage was set at 50 V. During laser and TIG melting, a continuous flow of argon (~ 10 l/min) was applied onto the specimen surface to protect the melted region from oxidation and undesirable contamination.

After laser melting, transverse sections were obtained from each processed zone and standard method of metallography was followed for microstructure analysis and microhardness measurement. Optical microscopy, scanning electron microscopy of type LEO 1430 VP and X-ray diffraction were used for this investigation. In order to obtain a melt width sufficient for X-ray diffraction, the laser beam scan was overlapped by about 50% of the beam size.

3. Results and discussion

3.1. Laser melting

3.1.1. Dimensions and morphology of the melted zone

Table 1 illustrates the melted depth, melted width and the average microhardness of nodular cast iron after laser melting treatment using different power densities and pulse durations. These measurements were made on polished and etched transverse cross-sections at the mid-width of each sample. The reported microhardness values in Table 1 are the average of 5–10 measurements taken at different locations in the melted zone for each specimen. Processing conditions which

involve low power density (80 MW/m^2) and short pulse duration (0.8 ms) resulted in a wide melt zone (~ 0.67 mm) and of a little penetration (0.1 mm) with a relatively low hardness (560 HV) while high power density (>300 MW/m^2) and relatively longer pulse duration (2.5 ms) produced deep (~ 0.35 mm) and narrow melted zone (0.45 mm) and of relatively a high hardness (600 HV).

3.1.2. Microstructure and X-ray diffraction

The starting microstructure of the nodular cast iron consists of graphite nodules surrounded by ferrite and some amount of pearlite. The average microhardness of the unprocessed material was ~ 150 HV. A typical cross-section of laser-melted nodular cast iron processed at a low power density 80 MW/m^2 and a short pulse duration 0.8 ms is shown in Fig. 1a. There is a complete dissolution of the graphite nodules and re-solidification of the dendritic structure; some needle-like structure of irregular shape is also observed at the interface and in random locations of the melted zone. In the region at the bottom of the melt layer, only partial dissolution occurred. Also visible in this figure is the irregular shape of the interface, which is seen in all the laser-melted specimens. This can be interpreted as the melt layer encroached into the substrate. It was the material in the vicinity of the graphite nodules, which melted initially; this occurs, because of carbon enrichment near the graphite nodules locally lowers the melting point of the ferrous area. Examination of the melted zone at high magnification using a high resolution scanning electron microscopy showed a dendritic structure throughout the melt (Fig. 1b). These dendrites are characterized by long primary and secondary arms; the secondary arm spacing (DAS) was less than 0.5 μm , which indicates a considerable amount of a high cooling rate during solidification. Examination of the interior of this dendrite at high magnification did not show any distinctive feature such as martensite or pearlite (Fig. 1d).

Fig. 2a shows another transverse section of the laser-melted zone processed at a high power density (300 MW/m^2) and pulse duration 2.5 ms. The melted depth was 0.35 mm, which is three times deeper than the previous sample. The microstructure of this melted zone is relatively coarse dendritic compared with the dendrites seen in the previous specimen (DAS = 2–3 μm). SEM examination at high magnification reveals a martensitic structure within these dendrites (Fig. 2b).

Table 1
Dimensions and average hardness of laser-melted cast irons processed at different conditions

Specimen no.	Power density (MW/m^2)	Pulse duration (ms)	Scanning speed (mm/s)	Melted depth (mm)	Melted width (mm)	Average hardness (HV)
1	60	0.8	1.0	0.08	0.67	540
2	80	0.8	1.0	0.10	0.67	560
3	100	0.8	1.0	0.13	0.76	600
4	300	2.5	1.0	0.300	0.34	590
5	350	2.5	1.0	0.380	0.45	600

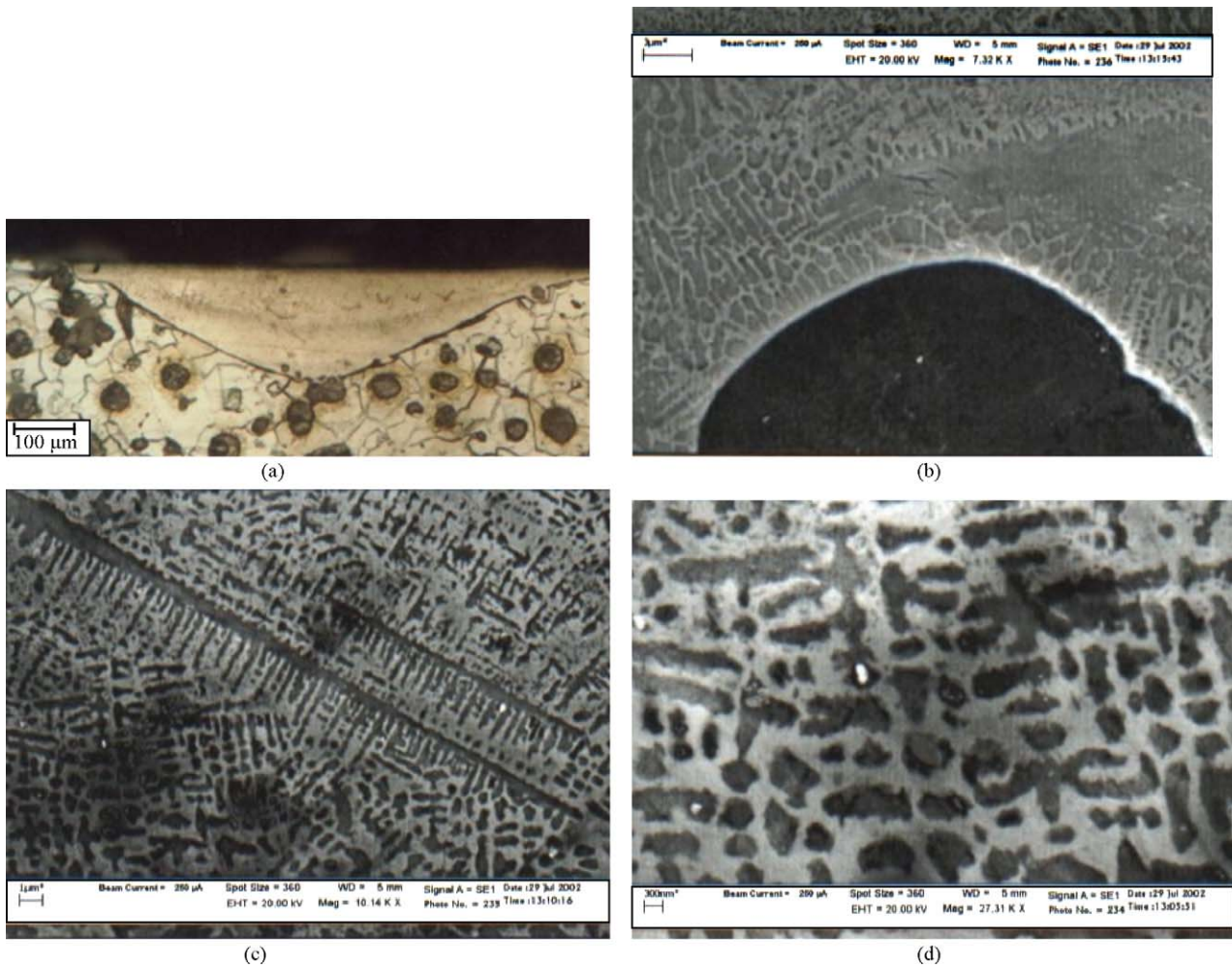


Fig. 1. (a) Optical micrograph shows transverse section of the laser-melted zone processed at (99.62 W/mm² per pulse, 0.8 ms pulse duration, 1 mm/s sample scanning speed), (b) SEM micrographs show the microstructure of the laser-melted zone of the lower part of (a) and (c and d) SEM micrographs show the microstructure of the central part of the laser-melted zone.

Fig. 3a and b shows X-ray diffraction peaks obtained from the specimen before and after laser melting, respectively. Before laser melting most of the peaks were indexed as α -bcc and cementite Fe₃C (Fig. 3a), but after laser melting, most

of the peaks correspond to γ phase (fcc) and Fe₃C (Fig. 3b), and traces of α .

From X-ray analysis of the laser-melted zone, two important results are obtained. Firstly, the austenite phase in the

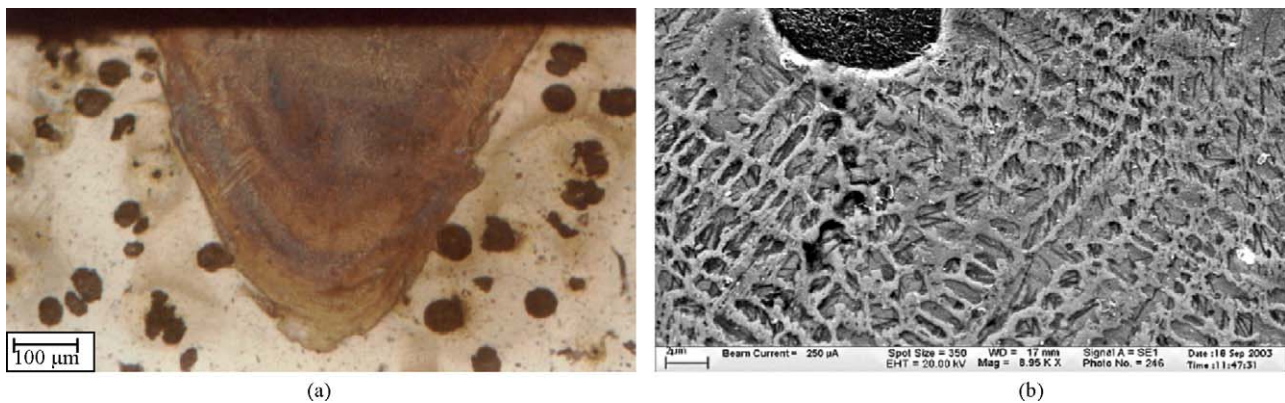


Fig. 2. (a) Optical micrograph shows transverse section of the laser-melted zone processed at (300 W/mm² per pulse, 2.5 ms pulse duration, 1 mm/s sample scanning speed) and (b) SEM micrographs show the microstructure of the laser-melted zone of the lower part of (a).

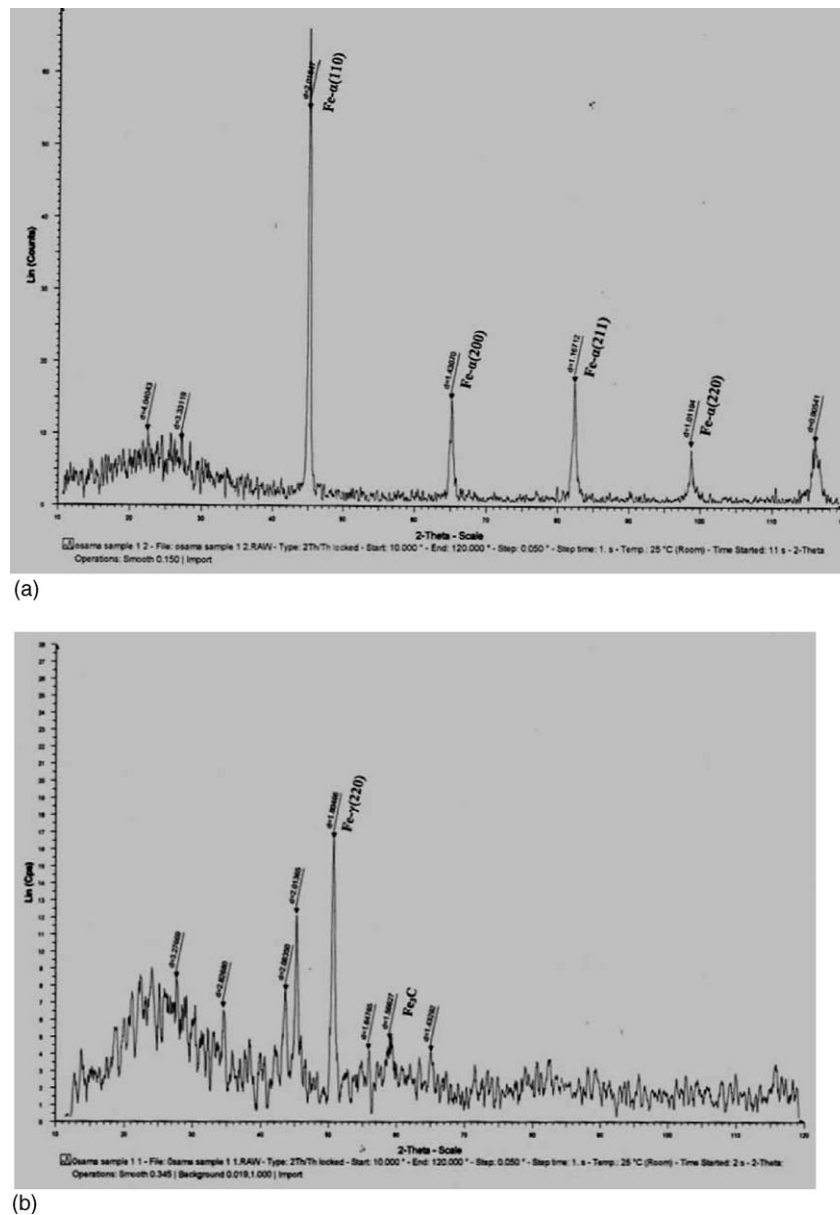


Fig. 3. X-ray diffraction pattern taken from the surface of nodular cast iron: (a) before laser melting and (b) after laser melting.

laser melt zone contained approximately 1.7 wt.% C, as calculated from the following equation relating austenite lattice parameter and carbon content [7]: $a = 0.3548 + (0.0044)x$, where a is the fcc lattice parameter in nanometer which is 0.6 nm (from the X-ray diffraction) and x is the weight percentage of carbon in solid solution. This carbon composition is consistent with the phase diagram for a modestly supercooled iron of near eutectic composition [1], and this helps explain why the austenite matrix is retained at room temperature. Secondly, the austenite {200} peak intensity was much more intense than the {111} peak. Since, in a randomly oriented austenitic material the {111} peak should have about twice the intensity of the {200} peak, this indicates that there is a preferred $\langle 100 \rangle$ austenite dendrite growth

direction, which is agreement with what is usually observed for fcc metals [7], with the $\langle 100 \rangle$ fcc direction normal to the surface.

3.2. Surface-melted nodular cast iron by TIG

Table 2 shows the parameters used for surface melting by TIG. At a constant voltage, increasing the current leads to an increase in the heat input and consequently increases the melted depth and width. Generally, the melted zone size in the specimen processed by TIG is far deeper and wider than those obtain by the laser beam process. Microstructure examination of the entire melted zone shows the same features with an increase in the scale of the microstructure with

Table 2
Dimensions and the average microhardness of the melted zone produced by TIG

Current (A)	Voltage (V)	Melted depth (mm)	Melted width (mm)	Average hardness (HV)
80	50	0.7	6.6	700
100	50	0.88	7	725
120	50	1.2	7.7	725
160	50	1.68	8.5	750

increasing the current. Fig. 4a shows a typical transverse section of the melted zone processed by TIG at 120 A and 50 V. The melted zone was 1.2 mm deep and 7.7 mm wide, which is nearly eight times larger than the melted zone produced by laser beam. A dendritic structure of typical white cast iron was seen in all the melt except near the interface where partial dissolutions observed. The interior of these dendrites displayed hypereutectic structure comprising coarse cementite and fine pearlite (appeared gray in the micrograph). The interdendritic regions showed a mixture of eutectic consisting of transform austenite (gray) and a thick layer of cementite (white) (Fig. 4b). The measurements of microhardness in several places in the melted zone showed higher values (600–750 HV) compared to those processed by the laser beam.

In the specimen melted by TIG, the size of the melted zone was enough for X-ray diffraction, which showed several high intensity peaks indexed as Fe_3C . No retained austenite was found.

The difference in the microstructures and microhardness between laser-melted specimens and TIG-melted specimens can be explained on the basis of different cooling rates. Due to the small melted volume of the laser-melted specimens as compared with the large volume of the melt produced by the TIG for the same materials thickness (1/2 in.), a very high cooling rate was associated with laser melting. Solidification of the nodular cast iron under low cooling rates (as in the TIG) commences with the crystallization of austenite.

Due to the limited solubility of carbon in austenite, the last liquid became rich in carbon and reached the eutectic point to form ledeburite (austenite + graphite). On further cooling carbon solubility in austenite decreased with decreasing temperature and more graphite was formed. When the temperature reaches the eutectoid temperature (723°C) the austenite transformed to pearlite. This path of solidification produces mainly graphite nodules in a matrix of pearlite. In the case of laser melting, the high cooling rate causes austenite to crystallize as primary dendrites. The last liquid will be enriched in carbon and form a eutectic of austenite and cementite. The eutectic was a divorce type because the eutectic austenite formed on the primary austenite leaving cementite surrounding the austenite dendrites. On further cooling to room temperature, the austenite may transform partially to martensite depending on the M_s temperature (i.e. martensite start temperature). In the present investigation, the high concentration of carbon dissolve in the austenite (1.7%) led to depression of the M_s and M_f temperatures below room temperature leading to a high proportion of retained austenite at room temperature. The melted zone processed by TIG experienced a relatively lower cooling rate and this would give more time for the carbon to precipitate within the austenite dendrites as shown in Fig. 4b. The remaining austenite had a lower amount of dissolved carbon and transformed to pearlite.

4. Conclusions

Surface melting of nodular cast iron by ND-YAG laser beam of maximum power 100 W leads to dissolve most of the graphite nodules and re-solidification of a fine dendritic structure comprising retained austenite as well as some martensite and cementite Fe_3C . The maximum melted depth for laser processing used was 0.5 mm and maximum hardness ranged between 500 and 600 HV.

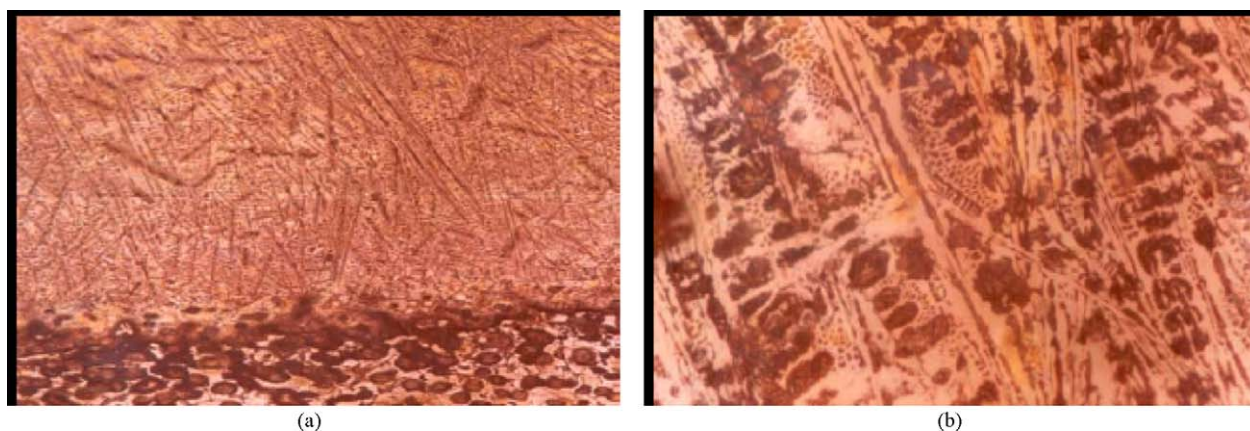


Fig. 4. (a) Optical micrographs show the cross-section of melted zone of nodular cast iron produced by TIG (magnification 110 \times) and (b) optical micrograph of melted zone (magnification 1100 \times).

Surface melting of nodular cast iron by TIG operated at 120 A and 50 V produced a maximum melt depth of 1.68 mm and 750 HV. The microstructure was dendritic consisting of transformed austenite in a matrix of austenite and cementite Fe_3C .

In laser-melted specimens, there was a substantial amount of retained austenite, which contained a high concentration of dissolved carbon and showed preferred growth on [1 0 0] direction. In TIG-melted specimen, all the austenite is transform to a hyper eutectic structure. This difference in the microstructure was interpreted as due to the different cooling rates.

Acknowledgments

Acknowledgments are made to laser research center in Tripoli for their permission in using the laser, to the petroleum research center in particular to Osama Burshan, for the use of scanning electron microscopy and to industrial research center in Tripoli for the use of X-ray diffraction.

References

- [1] C.H. Chen, C.J. Alstetter, J.M. Rigsbee, Laser processing of cast iron for enhanced erosion resistance, *Metall. Trans.* 15A (1984) 719.
- [2] D.N. Trafford, T. Bell, J.C. Megaw, A.S. Bransden, Laser treatment of grey iron, *Met. Technol.* 10 (1983) 69.
- [3] N.B. Dahotre, *Lasers in Surface Engineering*, ASM International, Ont., Canada, 1998.
- [4] G. Christodoulou, A. Walker, D.R.F. West, W.M. Steen, Laser surface melting of some alloyed steels, *Met. Technol.* 10 (1983) 215.
- [5] J.D. Majumdar, I. Manna, Laser surface alloying of AISI 304 stainless steel with molybdenum for improving in pitting and erosion–corrosion resistance, *Mater. Sci. Eng.* 267 (1999) 50.
- [6] J.H. Abboud, D.R.F. West, Laser surface melting of Ti–10V–2Fe–3Al alloys, *J. Mater. Sci. Lett.* 11 (1992) 1322.
- [7] E.M. Breinan, B.H. Kear, C.M. Banas, *Superalloys, Metallurgy and Manufacture*, 3rd International Symposium, Seven Springs, PA, 1975.
- [8] R. Reed-Hill, *Physical Metallurgy Principle*, D. Van Nostrand Company, 1973.

Further reading

- [9] B.D. Cullity, *Element of X-Ray Diffraction*, Addison-Wesley, Reading, MA, 1978.